REPORT DOCUMENTATION PAGE

Form Approved OMB NO. 0704-0188

1. REPORT DATE (DD-MM-YYYY)	2. REPORT TYPE	3. DATES COVERED (From - To)
04-07-2008	Final Report	1-Mar-2005 - 29-Feb-2008

4. TITLE AND SUBTITLE
Final Report on the Dynamic Failure of Multi-layer MEMS at High Loading Rates: Experiments and Simulations

5a. CONTRACT NUMBER
W911NF-05-1-0063

5b. GRANT NUMBER

5c. PROGRAM ELEMENT NUMBER
611102

6. AUTHORS
John Lambros, Ioannis Chasiotis

5d. PROJECT NUMBER

5e. TASK NUMBER

5f. WORK UNIT NUMBER

7. PERFORMING ORGANIZATION NAMES AND ADDRESSES
University of Illinois - Urbana
Grants and Contracts Office
109 Coble Hall
Champaign, IL 61820 -6242

8. PERFORMING ORGANIZATION REPORT NUMBER

9. SPONSORING/MONITORING AGENCY NAME(S) AND ADDRESS(ES)
U.S. Army Research Office
P.O. Box 12211
Research Triangle Park, NC 27709-2211

10. SPONSOR/MONITOR'S ACRONYM(S)
ARO

11. SPONSOR/MONITOR'S REPORT NUMBER(S)
48421-EG.3

12. DISTRIBUTION AVAILIBILITY STATEMENT
Approved for Public Release; Distribution Unlimited

13. SUPPLEMENTARY NOTES
The views, opinions and/or findings contained in this report are those of the author(s) and should not contrued as an official Department of the Army position, policy or decision, unless so designated by other documentation.

14. ABSTRACT
Aims: Microelectromechanical Systems (MEMS) are increasingly used in critical military applications involving high loading rate for which failure modes can develop that are not present under static loading. We focused on understanding the dynamic failure response of multilayer MEMS at the material and structural scales. Findings/significance: We have performed static and dynamic failure experiments on polysilicon, and on Au and PZT/metal MEMS (from Army Research Laboratory.) The effects of loading rate, material, and geometry were studied. Findings show that failure modes are highly dependent on loading rate and geometry, and include material failure, structural failure or delamination. In addition, MEMS response may

15. SUBJECT TERMS
MEMS, thin films, dynamic failure, stress-strain curve, PZT, Au, Pt, multi-layer, Hopkinson bar, laser loading

16. SECURITY CLASSIFICATION OF:			17. LIMITATION OF ABSTRACT	15. NUMBER OF PAGES	19a. NAME OF RESPONSIBLE PERSON
a. REPORT	b. ABSTRACT	c. THIS PAGE			John Lambros
U	U	U	SAR		19b. TELEPHONE NUMBER: 217-333-2242

Report Title

Final Report on the Dynamic Failure of Multi-layer MEMS at High Loading Rates: Experiments and Simulations

ABSTRACT

Aims: Microelectromechanical Systems (MEMS) are increasingly used in critical military applications involving high loading rate for which failure modes can develop that are not present under static loading. We focused on understanding the dynamic failure response of multilayer MEMS at the material and structural scales. Findings/significance: We have performed static and dynamic failure experiments on polysilicon, and on Au and PZT/metal MEMS (from Army Research Laboratory.) The effects of loading rate, material, and geometry were studied. Findings show that failure modes are highly dependent on loading rate and geometry, and include material failure, structural failure or delamination. In addition, MEMS response may appear either ductile or brittle, depending on their components. Micro-tension experiments in the range 10^-6/s - 10 /s showed significant rate sensitivity in Au and Pt films, and failure initiation in the PZT layer of structures. Device level failure was investigated over almost 7 orders of magnitude of loading rate, from peak accelerations of 500g to 10^8g (g: acceleration of gravity), using a drop weight tower, a Hopkinson bar and a pulsed laser loading set-up. Results illustrated the mechanisms of energy transfer at the MEMS scale and the existence of multiple failure modes that depend not only on peak acceleration, but also on loading duration.

List of papers submitted or published that acknowledge ARO support during this reporting period. List the papers, including journal references, in the following categories:

(a) Papers published in peer-reviewed journals (N/A for none)

Kimberley J., Lambros J. and Chasiotis I., "Failure of Microelectromechanical Systems subjected to impulse loads", International Journal of Solids and Structures, Vol. 45, No. 2, pp. 497-512, 2008.

Number of Papers published in peer-reviewed journals: 1.00

(b) Papers published in non-peer-reviewed journals or in conference proceedings (N/A for none)

Number of Papers published in non peer-reviewed journals: 0.00

(c) Presentations

1. Kimberley J., Cooney R., Minary J.M., Chasiotis I. and Lambros J., "Dynamic failure of MEMS: Experiments and simulations", ASME winter annual meeting, Chicago IL, November 2006.

2. Lambros J., Kimberley J., Chasiotis I., Polcawich R., Pulskamp J., "Experimental Investigation of Failure of MEMS Subject to Stress Wave Loading", 17th US Army Symposium on Solid Mechanics, Baltimore, MD April 2-5, 2007.

3. Chasiotis I., Jonnalagadda K., Lambros J., Pulskamp J., Polcawich R. and Dubey M., "Strain rate dependent mechanical behavior of Au and Pt films for MEMS", SES Annual Technical Meeting, 2007.

4. Chasiotis I., Jonnalagadda K., Lambros J., Pulskamp J., Polcawich R. and Dubey M., "Strain Fields in Thin Metal Films for MEMS Subjected to Various Strain Rates", 2008 TMS Annual Meeting & Exhibition.

5. Lambros J., Kimberley J., Chasiotis I., Cooney R., Dubey M., Polcawich R. and Pulskamp J., "Dynamic Failure of Layered Micro Scale Structures", SEM International Congress and Exposition, Orlando, FL, June, 2008.

Number of Presentations: 5.00

Non Peer-Reviewed Conference Proceeding publications (other than abstracts):

Number of Non Peer-Reviewed Conference Proceeding publications (other than abstracts): 0

Peer-Reviewed Conference Proceeding publications (other than abstracts):

1. Kimberley J., Chasiotis I. and Lambros J., “Dynamic failure of microelectromechanical systems”, SEM conference and exposition, St. Louis, MO, June, 2006.

2. Tang X., Jonnalagadda K., Chasiotis I., Lambros J., Polcawich R., Pulskamp J. and Dubey M., “Effect of Strain-rate on the Mechanical Behavior of Pt-Films for MEMS”, SEM conference and exposition, Springfield, MA, June, 2007.

3. K. Jonnalagadda, I. Chasiotis, “Strain-rate dependent mechanical behavior of Au and Pt film for MEMS,” Proceedings of 44th Annual Technical Meeting of the Society of Engineering Science, College Station, TX, October, 2007.

4. Yagnamurthy S., Chasiotis I., Lambros J., Polcawich R., Pulskamp J. and Dubey M., “Mechanical Properties of PZT Films and their Composites for RF-MEMS”, SEM International Congress and Exposition, Orlando, FL, June, 2008.

Number of Peer-Reviewed Conference Proceeding publications (other than abstracts): 4

(d) Manuscripts

1. Cooney R.S., Kimberley J., Lambros J., Chasiotis I. and Barker N.S., “Failure of Au RF-MEMS Switches Subjected to Dynamic Loading”, submitted to Sensors and Actuators A: Physical, 2008.

2. Kimberley J., Lambros J., Chasiotis I., Polcawich R., Pulskamp J. and Dubey M., “Mechanics of energy transfer and failure of ductile microbeams subjected to dynamic loading”, submitted to Journal of the Mechanics and Physics of Solids, 2008.

3. K. Jonnalagadda, I. Chasiotis, J. Lambros, R. Polcawich, J. Pulskamp, and M. Dubey, “Experimental Investigation into the Strain Rate Dependent Mechanical Behavior of Nanocrystalline Pt Films”, submitted to Experimental Mechanics, 2008.

4. S. Yagnamurthy, I. Chasiotis, J. Lambros, R. Polcawich, J. Pulskamp, M. Dubey, “Mechanical Properties and Failure Initiation in PZT Films and their Composites for RF-MEMS”, in preparation for Journal of Microelectromechanical Systems, 2008.

5. Kimberley J., Lambros J., Chasiotis I., Polcawich R., Pulskamp J. and Dubey M., “Dynamic Failure of Metal MEMS Subjected to Intermediate Loading Rates”, in preparation for Journal of Microelectromechanical Systems, 2008.

6. Kimberley J., Lambros J., Chasiotis I., Polcawich R., Pulskamp J. and Dubey M., “Failure of Layered MEMS Across a Range of Dynamic Loading Rates”, in preparation for Experimental Mechanics, 2008.

Number of Manuscripts: 6.00

Number of Inventions:

Graduate Students

NAME	PERCENT SUPPORTED
Jamie Kimberley	0.75
Robert Cooney	1.00
Sivakumar Yagnamurthy	1.00
Krishna Jonnalagadda	0.25
FTE Equivalent:	**3.00**
Total Number:	**4**

Names of Post Doctorates

NAME	PERCENT SUPPORTED
FTE Equivalent:	
Total Number:	

Names of Faculty Supported

NAME	PERCENT_SUPPORTED	National Academy Member
John Lambros	0.10	No
Ioannis Chasiotis	0.10	No
FTE Equivalent:	**0.20**	
Total Number:	**2**	

Names of Under Graduate students supported

NAME	PERCENT_SUPPORTED
FTE Equivalent:	
Total Number:	

Student Metrics

This section only applies to graduating undergraduates supported by this agreement in this reporting period

The number of undergraduates funded by this agreement who graduated during this period:	0.00
The number of undergraduates funded by this agreement who graduated during this period with a degree in science, mathematics, engineering, or technology fields:.....	0.00
The number of undergraduates funded by your agreement who graduated during this period and will continue to pursue a graduate or Ph.D. degree in science, mathematics, engineering, or technology fields:.....	0.00
Number of graduating undergraduates who achieved a 3.5 GPA to 4.0 (4.0 max scale):	0.00
Number of graduating undergraduates funded by a DoD funded Center of Excellence grant for Education, Research and Engineering:	0.00
The number of undergraduates funded by your agreement who graduated during this period and intend to work for the Department of Defense	0.00
The number of undergraduates funded by your agreement who graduated during this period and will receive scholarships or fellowships for further studies in science, mathematics, engineering or technology fields:	0.00

Names of Personnel receiving masters degrees

NAME	
Robert Cooney	
Total Number:	**1**

Names of personnel receiving PHDs

NAME	
Jamie Kimberley	
Krishna Jonnalagadda	
Total Number:	**2**

Names of other research staff

NAME	PERCENT_SUPPORTED
FTE Equivalent:	
Total Number:	

Sub Contractors (DD882)

Inventions (DD882)

Final Report

Dynamic failure of multi-layer MEMS at high loading rates: Experiments and simulations

(ARO Proposal No. 48421-EG)

Start Date: March 1, 2005

PI: John Lambros, co-PI: Ioannis Chasiotis
Aerospace Engineering
University of Illinois at Urbana-Champaign, Urbana IL 61801

ABSTRACT

Aims: Microelectromechanical Systems (MEMS) are increasingly used in critical military applications involving high loading rate for which failure modes can develop that are not present under static loading. We focused on understanding the dynamic failure response of multilayer MEMS at the material and structural scales. Findings/significance: We have performed static and dynamic failure experiments on polysilicon, and on Au and PZT/metal MEMS (from Army Research Laboratory.) The effects of loading rate, material, and geometry were studied. Findings show that failure modes are highly dependent on loading rate and geometry, and include material failure, structural failure or delamination. In addition, MEMS response may appear either ductile or brittle, depending on their components. Micro-tension experiments in the range 10^-6/s - 10 /s showed significant rate sensitivity in Au and Pt films, and failure initiation in the PZT layer of structures. Device level failure was investigated over almost 7 orders of magnitude of loading rate, from peak accelerations of 500g to 10^8g (g: acceleration of gravity), using a drop weight tower, a Hopkinson bar and a pulsed laser loading set-up. Results illustrated the mechanisms of energy transfer at the MEMS scale and the existence of multiple failure modes that depend not only on peak acceleration, but also on loading duration.

TABLE OF CONTENTS

List of Figures

Figure 13: SEM micrographs of the Full Stack (SiO2/TiPt/PZT/Pt) beams: **(a)** before loading, after loading in SHPB with peak accelerations approximately **(b)** 100,000g, **(c)** 200,000g, and **(d)** 300,000g.

Figure 14: Time sequence showing the deformed geometry of the Full Stack array loaded in the SHPB to a peak acceleration of 100,000g.

Figure 15: Failure rate as a function of peak applied acceleration across several orders of magnitude of applied load. An 83% versus a 50% (diamond symbol) failure rate at the highest acceleration is obtained counting failure over the entire chip or only over the surviving MEMS arrays, respectively.

Key outcomes of this Research Project

- ***The response of Pt and Au films was investigated from 10^{-7} s^{-1} to 10 s^{-1}. This represents an increase by 4 orders of magnitude over what is available in the literature.***
- ***We were also able to determine strain rates (20 s^{-1}) beyond which plasticity did not play a role in Pt and Au films until we reached the film mechanical strength.***
- ***The mechanical behavior of PZT thin films was not documented before this research. The elastic limit of PZT is 252±6 MPa and failure in the PZT composites initiates in the PZT layer at 250 MPa. Therefore, for all design purposes the PZT layers should not be exposed to stresses near 250 MPa, or otherwise their performance will be degraded over many loading cycles.***
- ***A contact and momentum transfer mechanism was responsible for the large deformations observed in dynamic loading of metal microbeams. The details of the support for such ductile material, where failure did not occur, were not very significant in terms of beam loading. Additionally, viscous damping effects were found to be dominant in determining the final deformed shape of the beams.***
- ***In intermediate rate dynamic experiments both the peak acceleration and loading duration, as well as details of the load history profile, were seen to influence failure.***
- ***The results of this study establish the severity of dynamic failure in MEMS, despite their small mass, and its dependence on the level of acceleration which spanned about 7 orders of magnitude.***
- ***From this research effort, 1 journal paper has appeared in print, 3 have been submitted for publication and 3 are in preparation.***

Accomplishments (over all years)

Our approach involved a close coupling of experiments and simulations. *Input experiments* were performed to obtain material and interface failure properties. The phenomena observed in the input experiments dictated the complexity of the simulations so that all experimental observations were accounted for. For slow and intermediate rates a combination of *in situ* high-resolution optical microscopy coupled with Digital Image Correlation (DIC) was used. In addition, novel experimental techniques were developed, based on high strain rate laser pulse loading, a split Hopkinson bar and a drop weight tower, to study the MEMS response under dynamic loading. *Validation experiments*, performed at the entire device level were then used to compare with results from simulations.

Quasi-static strain rate experiments: The UIUC group had in the past pioneered the investigation of rate dependence of metallic thin films by designing and building in house a combination of a high-resolution optical microscope together with a microtensile tester capable of loading the metallic MEMS at controllable strain rates. The device was initially capable of providing reliable experimental data at strain rates from 10^{-6} /s to 10^{-3} /s. The device involves gripping and pulling a MEMS specimen, as shown in Figure 1 on the left, and taking real time optical images of the deformation process at 200× magnification with a CCD camera with 1024 × 768 pixel resolution and 15 fps frame rate, while imaging areas of 480 × 360 μm^2. In order to compute specimen strain with the aid of Digital Image Correlation (DIC), a random speckle

pattern was generated on the specimen surface by dispersion of a silicon powder with average particle size of 1 μm, as shown on the right side of Figure 1.

A major accomplishment of the present work is that the PIs have extended the original testing method by several orders of magnitude of strain rate, from 10^{-7} all the way up to 10 s^{-1}. This represents an increase by 4 orders of magnitude over what is available in the literature. ***Note that we were also able to determine strain rates (20 s^{-1}) beyond which plasticity did not play a role in Pt and Au films until we reached the film mechanical strength.*** This new experimental method involves the deposition of a finer pattern on the specimen surface and the coupling of a high speed camera capable of framing at rates of up to 100,000 frames per second with the 200× microscope. Using this pattern and our newly developed apparatus we were able to ***monitor failure at the time scale of tens of microseconds,*** as seen in the image sequence of Figures 2(a-c). This method allowed the measurement of full-field deformations for the first time at the scale of MEMS in the transverse and the axial directions, Figures 3(a,b). From those full-field measurements we extracted the homogeneous properties of the materials tested in this research program, Figures 3(c,d).

By this method, 400-nm thin nanocrystalline Pt specimens were tested in uniaxial tension at strain rates between 10^{-6} - 1 s^{-1}, see Figure 4(a). The elastic and inelastic mechanical properties, i.e. elastic modulus, Poisson's ratio, elastic limit, yield strength, and ultimate tensile strength and strain varied by a factor of two over the entire range of strain rates, see Figures 4(b,c) which points out to the important realization that at the scale of MEMS failure properties of metallic films vary strongly with strain rate and it is important that thorough experiments are conducted at all possible strain rates. The elastic modulus was constant with strain rate with an average value of E= 182 ± 8 GPa and the Poisson's ratio was measured as $\nu = 0.41$. Both elastic constants matched those of bulk Pt. The yield and tensile strengths of the Pt films were an order of magnitude higher than annealed bulk Pt, which renders ***these Pt films very appropriate for high stress applications.***

We also completed experiments on the mechanical response of PZT multi-layers fabricated by the ARL at Adelphi, MD. ***The mechanical behavior of PZT thin films was not documented before this research.*** We begun with the simplest component of the PZT stack, i.e. SiO_2 and obtained its elastic and fracture properties in a very repeatable fashion, see Figures 3(c,d). Then we conducted experiments with stacks of thin film stacks fabricated consisting of combinations of Oxide (Ox), Titanium (Ti), Platinum (Pt) and PZT. The specimens were stacks of Ox-TiPt-PZT-Pt, Ox-TiPt-PZT, Ox-TiPt and individual Ox and Pt thin films, with gauge length of 1000 microns and width of 50-100 microns, see Figure 5(a). The composite mechanical properties of the PZT stacks were computed from the stress vs. strain plots, while the mechanical properties of the individual PZT films were computed from those of the PZT stack and individual layer properties of Ox and TiPt thin films by using lamination theory. ***A major conclusion is that the elastic limit of PZT is 252±6 MPa and that failure in the PZT composites initiates in the PZT layer at 250 MPa stress, Figure 6.*** This was the case both with and without a Pt layer deposited at the top side of the composite PZT stack, Figures 5(b,c). ***Therefore, for all design purposes the PZT layers should not be exposed to stresses near 250 MPa, or otherwise their performance will be degraded over many loading cycles.***

Dynamic loading experimental technique development: We have developed a novel experimental method for dynamic testing of MEMS materials and devices. A high power pulse Nd:YAG laser (peak power 1 J, pulse duration 15 ns) is used to launch a stress wave in the Si

substrate of the MEMS. Upon reflection from the free surface the stress wave produces large tensile loads (up to 2 GPa) in sufficiently short times (accelerations up to 10^9 g, g: acceleration of gravity) to fail the MEMS dynamically. In addition, we developed techniques for intermediate dynamic loading of MEMS devices based on a drop weight tower (peak accelerations 500g to 3,500g) and a modified split Hopkinson Pressure bar (peak accelerations 30,000g to 300,000g). Overall, the devices we developed can load MEMS with peak accelerations over 7 orders of magnitude. We developed the novel dynamic loading devices using polysilicon MEMS. In the process we discovered important new phenomena in the dynamic failure of MEMS. We qualitatively observed three different failure modes that depend on loading rate, geometry and material: (a) Material fracture (Figure 7), (b) Delamination between layers (Figure 7), and (c) Debonding from Si substrate (Figure 8). We quantitatively studied the simplified geometry of a single pad made up of layers of polySi and SiO2 as a function of loading rate and geometry. Figure 9 presents postmortem SEM micrographs of laser loaded MEMS showing the evolution of damage for increasing amplitude of the applied stress pulse from 400 MPa to 1.2 GPa (15 ns duration for each), for a 9 micron tall pad made up of 3 layers of Si and 2 layers of SiO2. The failure starts at the corners (Figure 9a, top row) and progresses, with increasing load, to the scalloped feature in Figure 9b, top row, to the pyramidal failure made up of material fracture and delamination in Figure 9c, top row. The remainder of Figure 9 shows failure evolution for a 7 micron tall (Figure 9, middle row) and 2 micron tall (Figure 9, bottom row) pads at the same three loading rates. Clearly, failure is also a function of geometry and if the MEMS structures are smaller it is more difficult to cause failure since the inertial forces are smaller. However, a similar failure pattern is possible at a higher stress rate.

To complement the above experiments and extract local stress quantities, we have conducted a series of finite element simulations in which we simulated the actual MEMS geometry (obtained through detailed optical, SEM and AFM microscopy, and profilometry) subjected to the actual loading recorded experimentally. The simulations confirm that the location of crack initiation is the outer corner and show that in fact the crack initiates at the interface between the substrate and the first polysilicon layer – a fact which was subsequently confirmed experimentally.

ARL MEMS devices: Our effort then focused entirely on MEMS devices manufactured at ARL. Layered ceramic/metal MEMS devices manufactured at the Sensors and Electron Devices Directorate of the Amy Research Lab in Adephi, MD, were obtained. Extensive optical and SEM studies were done to determine the undeformed geometry of the devices. Figure 10 shows the combination of a large number optical micrographs illustrating a die with test structures, made up of different materials used in the ARL process.

***Device level high rate experiments and simulations*:** Using the pulsed Nd:YAG laser loading technique developed earlier in the project, we studied dynamic failure of the ARL MEMS devices. To achieve acceleration levels on the order of 10^9 *g* (*g*–acceleration due to gravity), Au MEMS devices were subjected to impulsive loads 40 ns in duration generated by a high power pulsed laser. Simple devices, such as cantilever and fixed-fixed beams of constant cross section were used in the experiments in order to facilitate comparison with companion finite element simulations. Figure 11 shows SEM images of the Au beams after loading at (a) $1x10^9$ *g*, and (b) $2x10^9$ *g*. Large beam deformation is seen as loading level increases. In addition, Si substrate failure is seen at the higher rate, although it is not known if this is subsequent to the main loading

event. Figures 12(a,b) also clearly shows the dependence of final deformed shape on beam length. In an effort to understand the mechanisms of energy transfer responsible for this severe beam deformation, we performed companion finite element simulations to investigate the effect of loading rate, boundary conditions, beam length, material constitutive response, and viscous damping on the deformation and final shapes of the beams. Simulation results were compared with the experimental observations to gain insight into the mechanisms responsible for impulsive deformation at the microscale. Figures 12(c,d) show predicted final deformed shapes as a function of length corresponding to experiments. Initially it was believed that the precise details of how the beam was attached to the substrate through the support would affect the amount of beam deformation by adjusting flexural waves that would travel along the beam. However, ***it was found that a contact and momentum transfer mechanism was responsible for the large deformations observed in postmortem inspection. The details of the support for such ductile material, where failure did not occur, were not very significant in terms of beam loading. Additionally, viscous damping effects were found to be dominant in determining the final deformed shape of the beams***, while rate effects in material response were found to be of lesser importance – although not negligible.

Device level intermediate rate experiments and simulations: To generate loading accelerations of the order of 100,000g's that are comparable to those in kinetic penetrator projectiles and other Army applications, we developed an experimental loading technique based on the split Hopkinson pressure bar (SHPB). A number of different specially designed fixtures were placed in the specimen region of the SHPB, and the dynamic loading generated by the projectile impact was channeled into the MEMS devices. Using appropriate fixtures, peak accelerations of 30,000g to 300,000g were achieved in the SHPB. In this loading range the mechanics of failure are different than the high rate case described above in that the MEMS devices have time to enter a resonant regime in which vibrational effects are possible. Figure 13 shows (a) undeformed, and postmortem SEM images of a cantilever array of the ARL manufactured active MEMS full stack (SiO2/TiPt/PZT/Pt) that has been loaded in the SHPB to peak accelerations of approximately (b) 100,000g (c) 200,00g and (d) 300,000g. Note that there is a progressive increase in damage (measured as number of beams failed) as rate increases up to about 200,000g, but there is less damage as rate is increased further to 300,000g. This phenomenon was investigated using companion FEA simulations and it was found that failure ultimately depends not only on peak acceleration, but also on the details of the loading history. Specifically, failure occurred much later in time in the lower loading cases, which changed the details of load history to which those MEMS had been subjected. Figure 14 shows, for example, an FEA simulation result for the 100,000g case that shows very large beam deformations later in the experiment. If the beams have not failed prior to that (as is the case in the 300,000g loading) many beams will fail at that point.

Loading across low to ultra-high loading rate range: An attempt was made to reconcile the results of the high and intermediate rate experiments. However it was not possible to do so with the ARL MEMS devices since the Au cantilever beams that failed in the laser loading experiments, did not show and failure in the SHPB loading, and the full stack arrays that failed progressively in the SHPB loading were completely destroyed by even the smallest laser induced load. Therefore, a different device material and geometry, Au RF MEMS switches manufactured at the University of Virginia, were used to compare failure evolution from low dynamic loads to

the highest dynamic loading possible in our lab. Three different experimental setups were used: a drop weight tower, which induced a maximum peak acceleration of 3,500*g* (*g*: acceleration of gravity), the Hopkinson pressure bar with a maximum peak acceleration of 300,000*g*, and the pulsed laser loading technique with a maximum peak acceleration of $1.8 \times 10^8 g$. In the drop weight tower the total load pulse duration was in the ms range and no failure of any kind occurred in the RF-MEMS devices or their substrate. At 90,000*g* (generated in the Hopkinson bar) no damage in either the substrate or the devices was observed. However, at 200,000*g* 10% of the switches failed although postmortem imaging showed no damage to the substrate. Damage increased after this acceleration and at 300,000*g* 20% of the switches failed, but, in addition, significant failure in the quartz substrate was recorded. Lastly, the pulsed laser loading technique was applied to accelerate the Au switches to $1.8 \times 10^8 g$, and the probability of failure at this loading ranged from 50% to 80%. At even larger accelerations, $10^9 g$, the probability of failure was 100%. Figure 15 shows failure probability as a function of peak acceleration loading. ***The results of this study establish the severity of dynamic failure in MEMS, despite their small mass, and its dependence on the level of acceleration which spanned about 7 orders of magnitude.***

Technology Transfer (over all years)

We have collaborated extensively primarily with the MEMS group at the Sensors and Electron Devices Directorate of the Amy Research Lab in Adephi, MD, throughout this entire project – from conception to sample design to testing to results dissemination. Specific instances of collaboration with ARL researchers include:

(a) During the planning stage of this project had contact with various Army researchers that manufacture and study MEMS. Drs. Dubey, Polcawich, Pulskamp and Currano (ARL, Sensors and Electron Devices Directorate, Adelphi, MD), Dr. Brown (ARL, Aberdeen Proving Ground, MD).

(b) On August 17, 2005, the two PIs of this project and Dr. Bruce LaMattina of ARO, organized a workshop on the "Dynamic failure of MEMS and thin films" at Crystal City, Arlington VA. There was a strong presence of several ARL researchers in the area of MEMS design and a keynote presentation was given by Dr. J. Pellegrino of ARL. The workshop resulted in a Proceedings CD with presentations by participants and a vision article by the PIs and Dr. Bruce LaMattina on critical issues in MEMS reliability.

(c) On August 18, 2005, both PIs visited the ARL Adelphi site for an all day meeting with L. Currano, M. Dubey, T.G. Brown, B. LaMattina, R. Polcawich, J. Pulskamp and E. Zakar. We gave detailed presentations of the capabilities of the UIUC labs and sought out areas of collaboration with ARL. It was decided at that meeting that we would design samples specifically for the dynamic experiments done here using materials of relevance to ARL.

(d) Over the course of the next several weeks we had many conference calls with R. Polcawich and J. Pulskamp to determine the type of blanket film samples to be manufactured, as well as the design of samples for quasi-static and dynamic experiments. These were shipped to UIUC and underwent testing. We closely interacted in the detailed design of standardized specimen

geometries for both quasi-static and dynamic MEMS testing. Two of the students involved in the project designed MEMS layouts that were sent to ARL for microfabrication.

(e) On December 7 2006, the two PIs of this project presented at the workshop on the mechanics of MEMS devices that was organized by Dr. Dubey of the ARL Adelphi MEMS group. The goal of the workshop was to present results from a few ARO/ARL funded projects on MEMS, including our own, and to discuss strategies for continuing research and fostering an even closer interaction between the Adelphi group and the academia researchers. Attending the meeting among others were Drs. B. LaMattina, M. Dubey, T.G. Brown and R. Polcawich. The PI's delivered detailed presentations of the research at UIUC and sought out areas of collaboration with ARL.

(f) The project co-PI, Prof. Chasiotis, and Dr. B. LaMattina of ARO co-organized a symposium on the "Dynamic Failure of MEMS" during the 2006 ASME International Mechanical Engineering Congress and Exposition in Chicago (November 2006).

(g) The transition of the test apparatus developed at UIUC for quasi-static testing to the Army Research Laboratory was requested on (12/07/2006) by Dr. Tusit Weerasooriya (AMSRD-ARL-WM-TD (B4600), Impact Physics Branch, Army Research Laboratory, Abedeen Proving Ground, MD 21005, Phone: (410)306-0969, E-MAIL: tusitw@arl.army.mil.) In January of 2008 Dr. Weerasooriya submitted a work order to UIUC to fabricate for his laboratory an apparatus similar to that developed by the UIUC group for the experiments conducted under this grant. Dr. Tusit Weerasooriya is visiting UIUC in August of 2008 to receive this apparatus.

(h) In June 2007 Dr. Jamie Kimberley, who received his Ph.D. under this project visited SEDD-ARL for technical discussions with the team there.

(i) On 14-15 of August 2007, Prof. Lambros and K. Jonnalagadda, a student of Prof. Chasiotis, attended the workshop "Fundamental of Robust and Reliable Nano/MEMS Structures and Devices", organized by ARL/ARO. During that time they presented discussions on the state-of-the-art understanding of failure of MEMS devices and future trends envisioned.

(j) On September 28, 2007, the co-PI Ioannis Chasiotis, had a day long visit with the ARL Adelphi MEMS group, and meetings with meeting with Drs. M. Dubey, P. Armitharaz, L. Currano, R. Polcawich, and J. Pulskamp. He also delivered and hour-long presentation with title "State of the Art and Challenges in Nanoscale Experimentation".

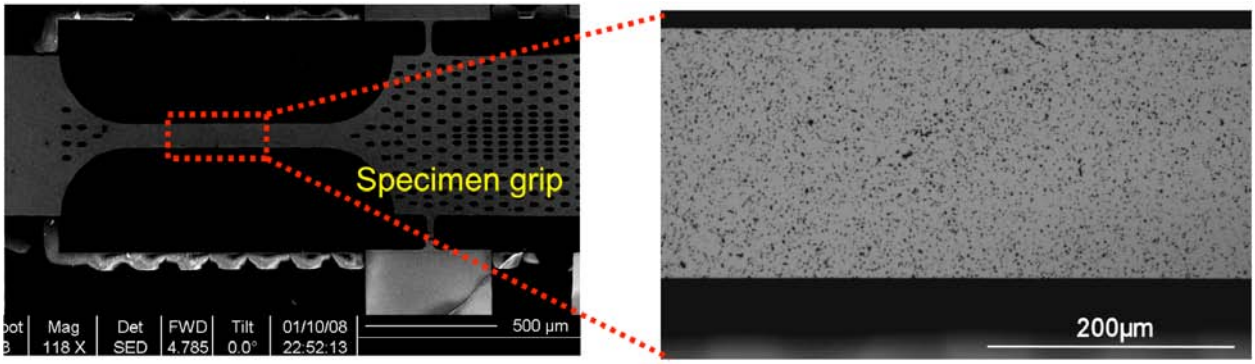

Figure 1: (Left) Unreleased dog-bone test specimen, (right) speckle pattern on the specimen gauge section deposited to measure full-field strains directly from the specimen surface.

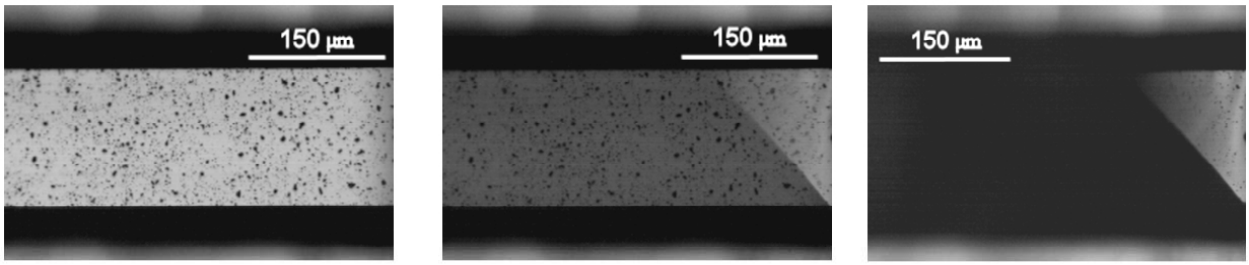

(a) **(b)** **(c)**

Figure 2: Optical images captured 1 ms apart at 10^{-2} s^{-1}. **(a)** Specimen before loading in tension, **(b)** crack emanating from the bottom edge of the specimen, and **(c)** complete specimen failure.

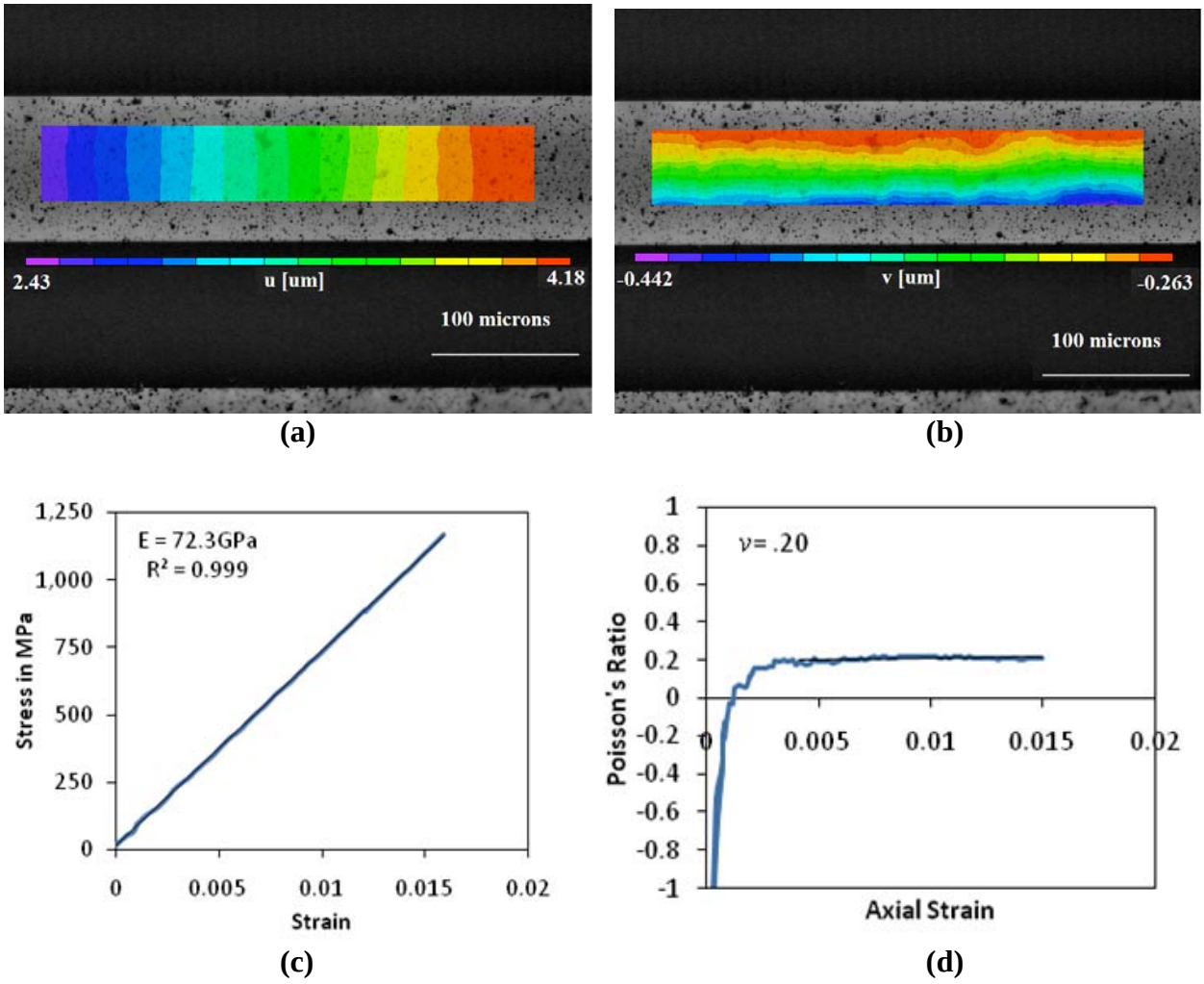

Figure 3: (a,b) Axial and transverse displacement field in a 100 micron wide SiO_2 specimen fabricated at ARL. **(c)** Stress vs. strain curve from the SiO_2 specimen whose deformation in shown in Fig. 3(a,b), **(d)** calculation of Poisson's ratio over the elastic regime of the stress strain curve.

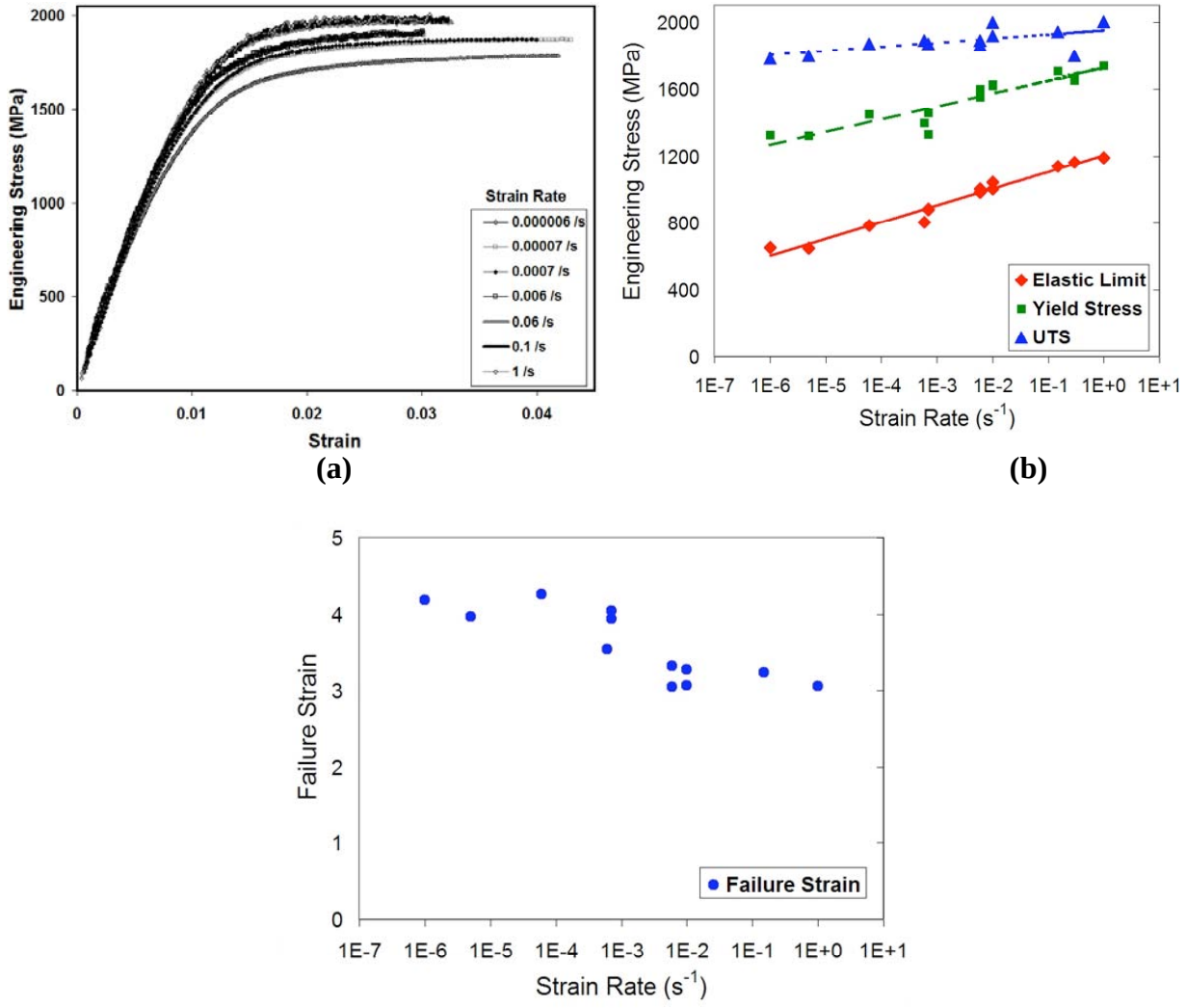

Figure 4: (a) Stress-strain curves of 400 nm Pt films tested in tension under a broad range of strain rates, **(b)** Elastic limit, yield stress, and ultimate tensile strength, and, **(c)** ultimate tensile strain of Pt films as a function of strain rate.

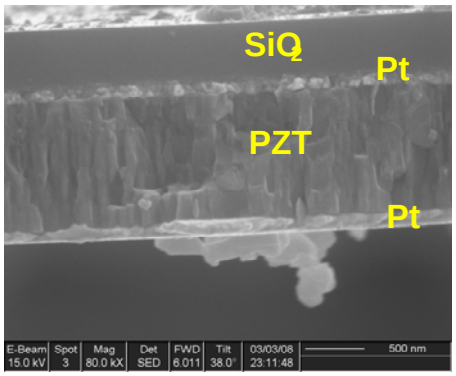

(a)

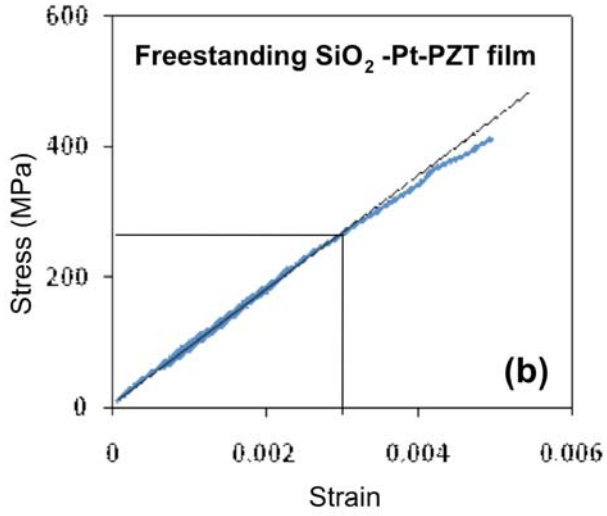

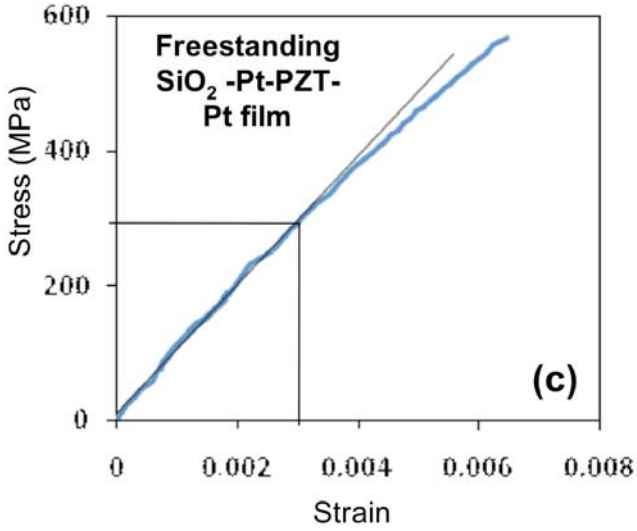

Figure 5: (a) Cross sectional image of SiO_2-Pt-PZT-Pt, **(b)** Stress-strain curve of freestanding SiO_2 -Pt-PZT film, **(c)** Stress-strain curve of freestanding SiO_2 -Pt-PZT-Pt film.

Material	Elastic modulus (GPa)	Failure stress (MPa)	Failure strain (%)	Elastic limit (%) strain	Elastic limit (MPa)
SiO_2	72.3±2	1046±200	1.4 ± 0.2		
Pt	173	1876 ± 10	3.84 ± 0.26	0.5	856 ± 46
SiO_2-Pt-PZT-Pt	93.5±6	511±50	0.6 ± 0.05	0.3	280±18
SiO_2-Pt-PZT	87.9±1	412±50	0.5 ± 0.05	0.3	263±3
PZT (Extracted)	**84±2**	460±35	0.5±0.1	**0.3**	**252±6**

Figure 6: Table with all results for the different PZT stacks and calculated properties of PZT itself.

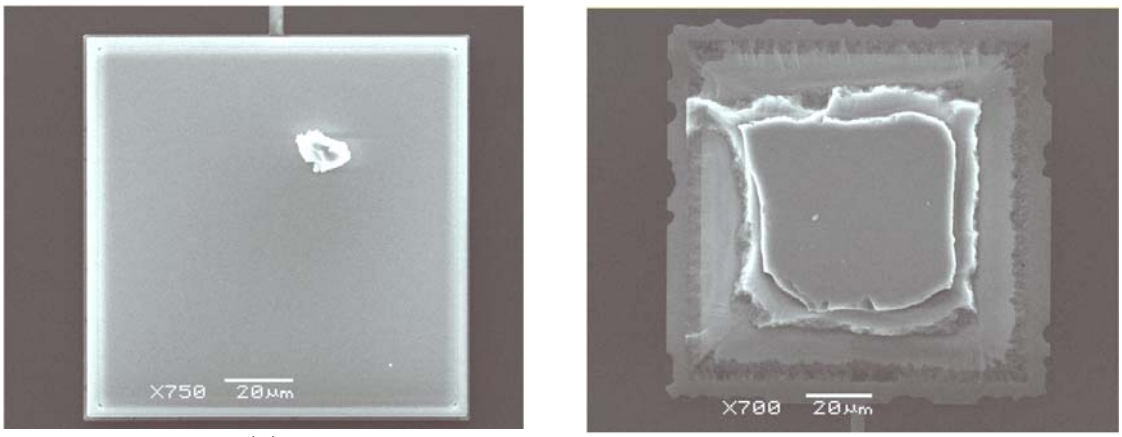

(a) **(b)**

Figure 7: SEM images **(a)** before and **(b)** after dynamic loading, showing material failure and interlayer debonding in a polysilicon MEMS device.

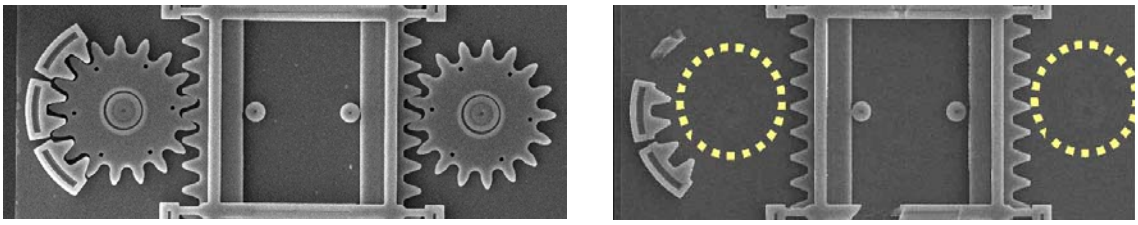

(a) **(b)**

Figure 8: SEM images **(a)** before and **(b)** after dynamic loading, showing substrate debonding (delamination) of gear shafts (inside dashed circles) in a polysilicon MEMS device.

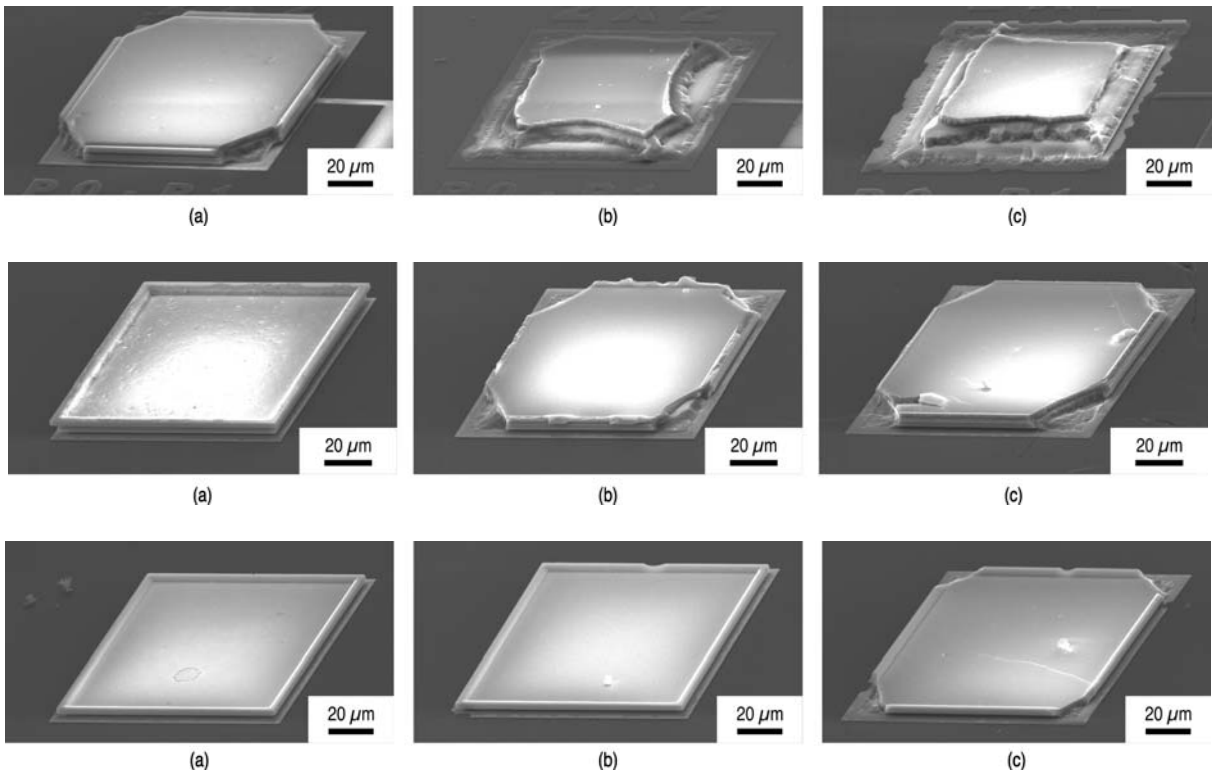

Figure 9: Post-mortem SEM images of tall (top row), medium (middle row) and short (bottom row) MEMS pads loaded dynamically with a peak stress of **(a)** 400 MPa, **(b)** 800 MPa, **(c)** 1200 MPa.

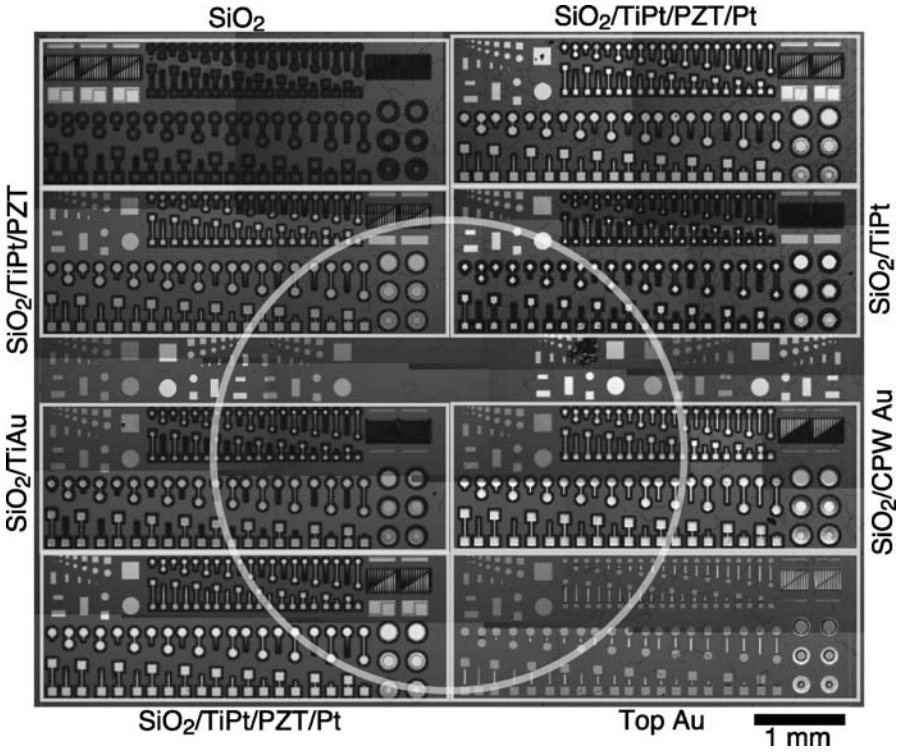

Figure 10: Layout of MEMS chip co-designed between UIUC and ARL containing the full stack devices (lower left) and a number of intermediate stage lay-ups.

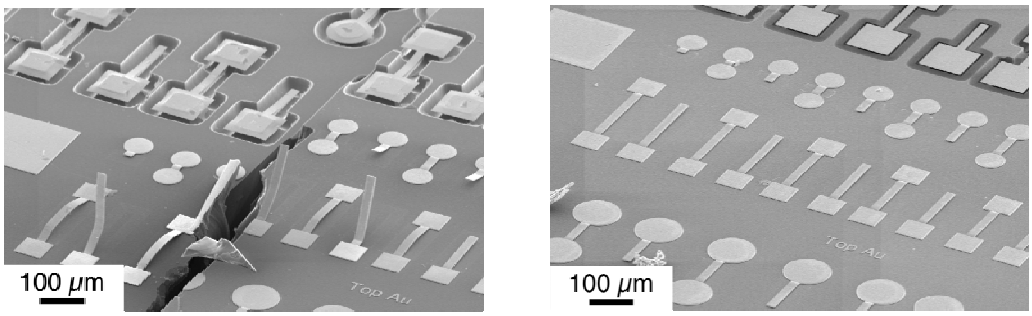

(a) **(b)**

Figure 11: Fixed-fixed and cantilever beams made of the Top Au layer after loading at **(a)** $1x10^9$ g, and **(b)** $2x10^9$ g.

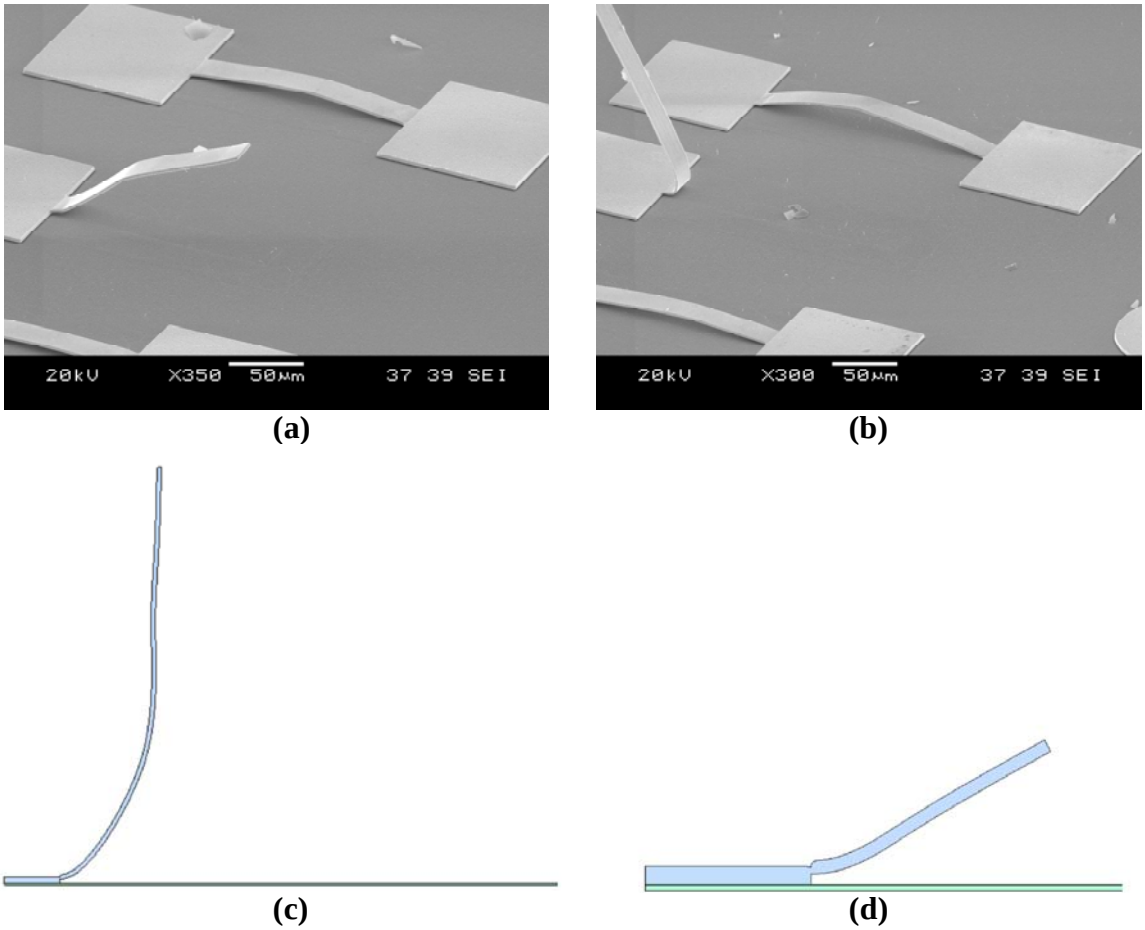

Figure 12: SEM images of deformed cantilever and fixed-fixed Au beams loaded at $2x10^9$ /s showing the dependence of deformation on beam length for **(a)** 200 m beams, and **(b)** 160 m beams. Corresponding final deformed shapes from companion finite element simulations are shown in **(c)** and **(d)** for 200 μm and 40 μm long beams, respectively.

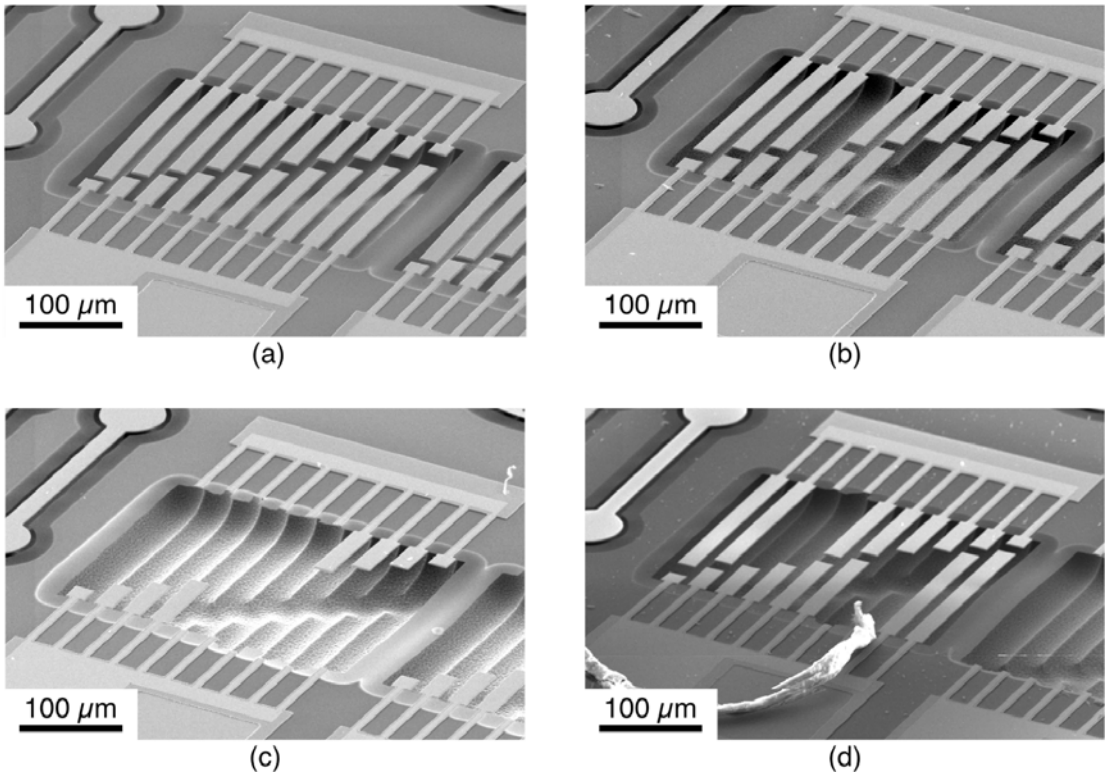

Figure 13: SEM micrographs of the Full Stack (SiO2/TiPt/PZT/Pt) beams: **(a)** before loading, after loading in SHPB with peak accelerations approximately **(b)** 100,000g, **(c)** 200,000g, and **(d)** 300,000g.

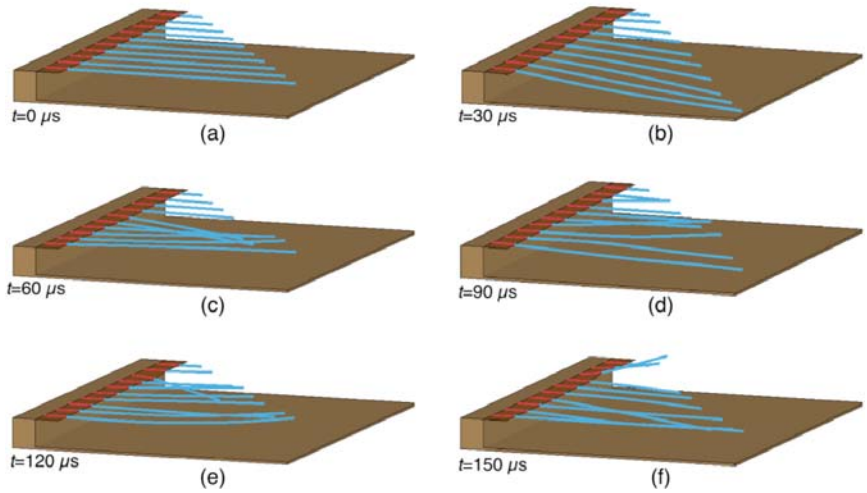

Figure 14: Time sequence showing the deformed geometry of the Full Stack array loaded in the SHPB to a peak acceleration of 100,000g.

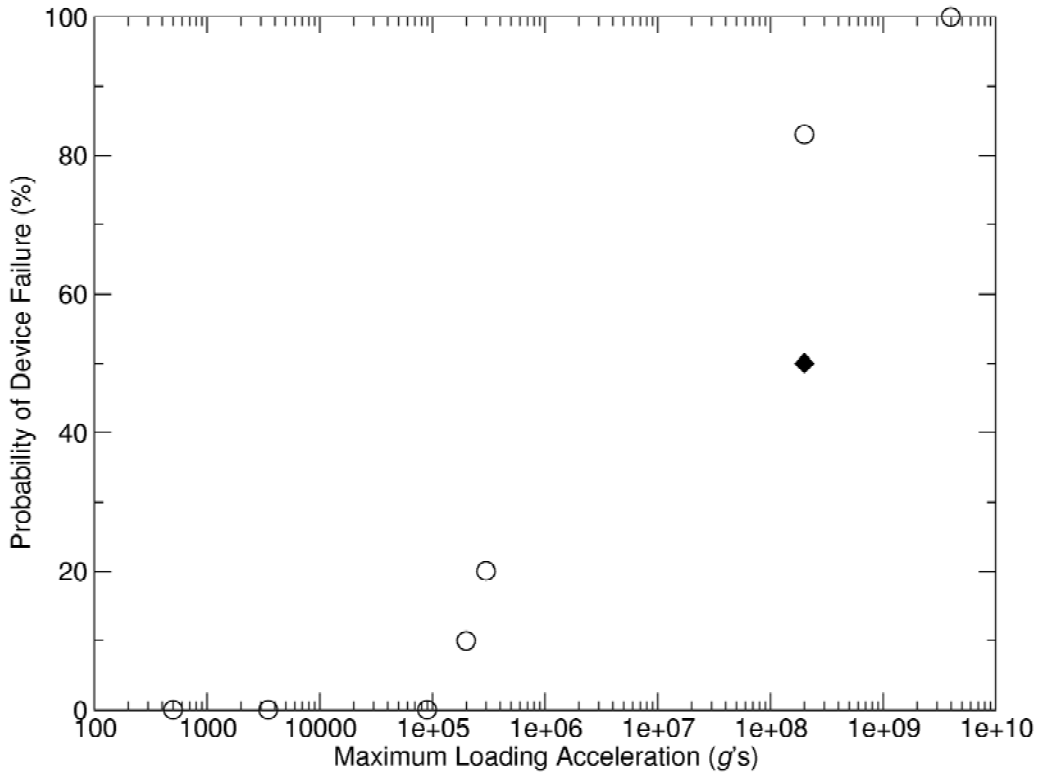

Figure 15: Failure rate as a function of peak applied acceleration across several orders of magnitude of applied load. An 83% versus a 50% (diamond symbol) failure rate at the highest acceleration is obtained counting failure over the entire chip or only over the surviving MEMS arrays, respectively.